



Fine-scale distribution of the lungworm *Halocercus delphini* in the lungs of the striped dolphin, *Stenella coeruleoalba*: implications about migration pathways and functional significance

Rachel V. Pool¹ | Neus Pons-García¹ | Francesco Consoli² | Miguel Rivero² | Cristiano Bombardi³ | Juan A. Raga¹ | Francisco J. Aznar¹

¹Marine Zoology Unit, Cavanilles Institute of Biodiversity and Evolutionary Biology (ICBiBE), Science Park, University of Valencia, Paterna, Spain

²Atlantic Center for Cetacean Research, University Institute of Animal Health and Food Security (IUSA), University of Las Palmas de Gran Canaria, Las Palmas, Spain

³Department of Veterinary Medical Science, University of Bologna, Bologna, Italy

Correspondence

Rachel V. Pool and Francisco J. Aznar, Marine Zoology Unit, Cavanilles Institute of Biodiversity and Evolutionary Biology (ICBiBE), Science Park, University of Valencia, Calle Catedrático José Beltrán 2, 46980 Paterna, Spain.
Email: rachel.pool@uv.es and francisco.aznar@uv.es

Funding information

Conselleria de Educació, Universidades y Empleo, Generalitat Valenciana, Grant/Award Number: Project AICO 2021/022; Biodiversity Foundation, MITECO, Grant/Award Number: VARACOMVAL

Abstract

Despite their high pathogenicity, limited knowledge is available on intrahost migration pathways and microhabitat distribution of pseudaliid lungworms. In this study, the distribution of *Halocercus delphini* in the lungs of the striped dolphin, *Stenella coeruleoalba*, was analyzed on three scales: between the right and left lungs, within the lungs, and between worm clusters. Evidence of a relationship between the distribution of *H. delphini* and the perfusion of the lungs of *S. coeruleoalba* is provided by the consistent correlation of these two factors, both on a longitudinal scale and by the difference in parasite burden between the left and right lung. This relationship, when coupled with the nested pattern of colonization, suggests that this species, like many other metastrongyloids, migrates to the lungs via the circulatory system. Additionally, the concentration of lungworms around the major airways could be a further reflection of the well-perfused nature of these passageways. Equally, this distribution could be a strategy to minimize the distance

Rachel V. Pool and Francisco J. Aznar contributed equally to this work.

This is an open access article under the terms of the [Creative Commons Attribution-NonCommercial-NoDerivs](https://creativecommons.org/licenses/by-nc-nd/4.0/) License, which permits use and distribution in any medium, provided the original work is properly cited, the use is non-commercial and no modifications or adaptations are made.

© 2024 The Authors. *Marine Mammal Science* published by Wiley Periodicals LLC on behalf of Society for Marine Mammalogy.

that larvae must travel to exit the lungs via the trachea, as do most other metastrongyloids. On a more localized scale, the tendency of *H. delphini* to form distinct heterosexual clusters even at low infection intensities indicates active mate-seeking behavior for reproduction.

KEYWORDS

cetaceans, *Halocercus delphini*, lungs, lungworms, microhabitat, Pseudaliidae, *Stenella coeruleoalba*, striped dolphin

1 | INTRODUCTION

The Pseudaliidae are a family of metastrongyloid lungworms almost exclusive to cetaceans, having been reported in ca. 29 odontocete species worldwide (Frajía-Fernández et al., 2016; Measures, 2001). Despite their name, pseudaliids can be found not only in the lungs, but also in the cranial sinuses, where heavy worm burdens can cause osseous lesions (Measures, 2001). In the lungs, severe infections have been linked to a variety of negative health effects on their hosts. For instance, lesions produced by *Torynurus convolutus* and *Pseudalius inflexus* in the harbor porpoise, *Phocoena phocoena*, led to secondary bacterial infections and the subsequent onset of pneumonia, which was recognized as the cause of death for ca. 50% of hosts examined in the North and Baltic Seas (Siebert et al., 2001). Likewise, verminous pneumonia caused by *Stenurus arctomarinus* was deemed a contributory factor in strandings of beluga whales, *Delphinapterus leucas* in Alaska (Burek-Huntington et al., 2015).

There is evidence that pseudaliids may use both trophic and direct transmission (e.g., lactogenic, transplacental) to infect their cetacean hosts (Pool, Chandradeva, et al., 2020). Therefore, an obvious question is the matter of how pseudaliids reach their final microhabitats where the adults are found. Despite numerous and extensive parasitological surveys of cetaceans (Mateu et al., 2014), we are not aware of any study that has addressed this question, nor one that has reported the detection of migrating larvae for any pseudaliid species. Other members of the Metastrongyloidea are known to use a variety of migration pathway(s) depending on the species, although those infecting the lungs typically use the adventitia of the arteries or the bloodstream to reach the lungs (Anderson, 2000). In pseudaliids, some observational data also suggest a link between the circulatory and the respiratory system in the case of *Pseudalius inflexus* which, on occasion, has been found in the heart and arteries of harbor porpoises, *Phocoena phocoena*, (Brosens et al., 1996; Geraci, 1979). However, whether lung-dwelling pseudaliids use the circulatory system as a migration pathway remains unexplored.

Another interesting issue that has never been investigated concerns the factors that drive the selection of specific microhabitats by lung-dwelling pseudaliids once the larvae have reached the lungs. In general, the distribution of helminths within organs can be accounted for by three major functional factors: (1) parasite specialization, which leads worms to select certain parts of the organ due to previous adaptations to a specific set of conditions; (2) competition, which may affect the spatial distribution of worms when a resource, e.g., food or space, is limited; and (3) the enhancement of mating opportunities, which can lead worms to aggregate in certain microhabitats to maximize sexual encounters (Holmes, 1990; Rohde, 1994). Two additional factors may affect worm distribution without necessarily impacting their fitness: the passive transport of worms within the organ by the host's physiology (Aznar et al., 2006; Lymbery, 1989), or the restriction of certain microhabitats as a side-effect of immune mechanisms (Holmes, 1990).

In this study, we examined the distribution of the pseudaliid, *Halocercus delphini*, in the lungs of the striped dolphin, *Stenella coeruleoalba*, with two major goals in mind. First, we focused on the relationship between the worm's distribution in the lungs and its potential migration pathway(s) through the circulatory system. To this end, we adopted an indirect approach using two spatial scales. On the one hand, we compared worm numbers

between the left and right lungs. In cetaceans, the cranial lobe is more pronounced and elongated in the right lung, which has an additional bronchus leading from the trachea, the *bronchus trachealis* (Kida, 1998; Piscitelli et al., 2013). The presence of this additional airway must increase blood perfusion in the right lung, and consequently increase its parasite burden if *H. delphini* uses the circulatory system to reach the lungs. On the other hand, in both lungs the number of bronchioles varies along the longitudinal axis (Nakakuki, 1994). This means that the number of arterioles, thus the relative blood perfusion, must also vary along the lungs' longitudinal axis. Thus, we tested whether the lung regions with a higher number of arterioles also had higher numbers of *H. delphini*.

The second goal of this study was to examine the microhabitat distribution of *H. delphini*. This dioecious parasite is very small (body length of males is ca. 5 mm; see Pool, Fernández, et al., 2020) and, therefore, our working hypothesis was that *H. delphini* should tend to occur in heterosexual aggregates to enhance mating opportunities (Lymbery, 1989; Rohde, 1994). To investigate this hypothesis, we selected “focal” worms across the lung and collected all surrounding individuals around them, if any. This allowed us to quantitatively assess the extent to which *H. delphini* individuals occur in aggregates, as well as the number of males and females of each aggregate.

2 | METHODS

2.1 | Lung data collection and infection parameters

Samples were obtained from a total of 120 striped dolphins that were found stranded along the Mediterranean coast of Spain (Valencian Community, between 40°31'00"N, 0°31'00"E and 37°50'00"N, 0°45'42"W) in the period 1987–2018. Only carcasses in preservation states 1–3 sensu Geraci and Lounsbury (2005) were selected for analysis. During necropsy the lungs were collected and frozen at –20°C. Lungs were thawed for 24 hr prior to analysis.

Except otherwise stated (see Sections 2.3 and 2.4 below), lungs were cut along the airways from the bronchus to the caudal apex, the parenchyma being examined macroscopically for the presence of lungworms. The lung tissue was also periodically rinsed throughout the dissection over a 0.2 mm sieve to wash away any blood obscuring worm detection. After dissection, the lung tissue was soaked in a tray and the water filtered through the sieve. The contents of the sieve were washed with saline into a Petri dish where they were then examined with a stereo microscope for further collection of nematodes. All fragments and whole worms were stored in 70% ethanol. Lungworms were examined under a light microscope and identified following Baylis and Daubney (1925), Gallego and Selva (1979), and Anderson (2009). Due to the tendency of *H. delphini* to form knots in the parenchyma with their anterior ends, lungworms were difficult to extract whole, and thus the total number of worms was estimated as the number of complete and/or incomplete worms with their caudal end intact.

Infection parameters are defined as in Bush et al. (1997) and Rózsa et al. (2000). “Prevalence” refers to the frequency of infected hosts, expressed as percentage; “intensity” is the number of worms in an infected host; “mean intensity” is the average number of worms per individual host in the subset of infected hosts; and “mean abundance” is the average number of worms per individual host considering all analyzed hosts, both infected and uninfected. To calculate 95% confidence intervals (CI), Sterne's exact method was used for prevalence and the bias-corrected and accelerated bootstrap method with 20,000 replications was used for mean intensity and abundance (Reiczigel et al., 2019).

2.2 | Comparison of right versus left lung

In a random sample of 19 dolphins, the right and the left lungs were weighed separately on a scale to the nearest 0.1 g, and their masses were compared using a paired *t*-test. Our expectation was that the right lung was heavier due to presence of its enlarged cranial lobe and the *bronchus trachealis* and, therefore, the test was one-tailed. Likewise, the number of worms between right and left lungs was compared with one-tailed Wilcoxon's paired test, using a sample of 94 dolphins.

Assuming that the potential difference of parasite loads between lungs are related to number of blood vessels and blood perfusion, we expected that the proportion of total worms in the right lung would remain constant at increasing intensity. We tested this hypothesis with generalized additive models (GAMs), which allowed us to fit a smoothed nonlinear function via penalized thin-plate regression splines (Wood, 2017). Since we dealt with proportions, a Beta regression distribution and a logit link function were used. The models were fitted based on the generalized cross-validation criterion (GCV), which controls for over-smoothing and automatically selects the effective degrees of freedom. Diagnostic plots of residuals were checked to examine model suitability (Wood, 2017).

2.3 | Worm distribution within the lung

In a sample of 14 dolphins, either the right or left lung was randomly selected and analyzed as described in Section 2.1, whereas the other lung (seven left and seven right) was used to describe the distribution of *H. delphini* within the lung. Each lung was first measured longitudinally and then pierced with a metal skewer wrapped in hemp cord; the skewer entered from the bronchus and followed its trajectory to exit at the caudal apex of the lung. After removing the skewer, the cord was left behind to mark its trajectory, and to act as a proxy for the bronchus in the parts of the lung where the bronchus had already separated into several smaller airways. The lung was then placed ventral-side down and cut laterally into ten slices of equal thickness, numbered 1 to 10, from the cranial to the caudal end (Figure 1). Using a transparent 5 × 5 mm circular grid, the distance was measured between the bronchus wall/the

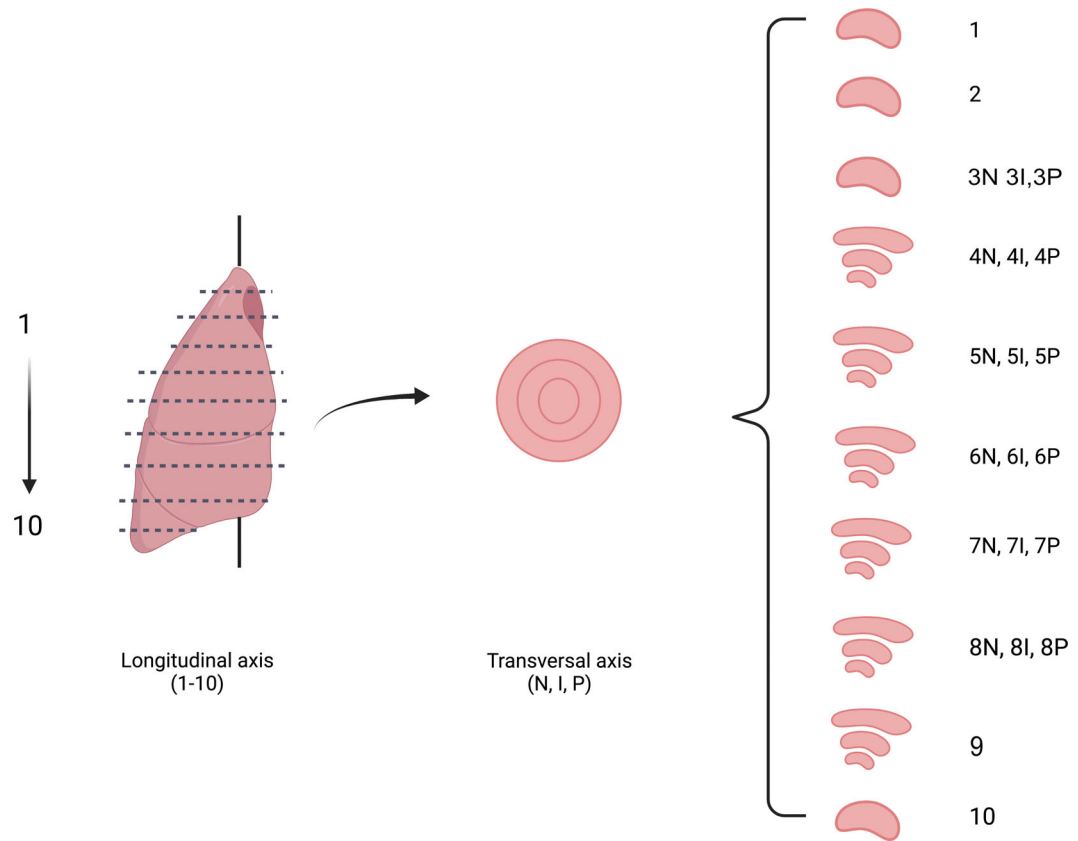


FIGURE 1 Schematic of the lung dissection protocol for the analysis of microhabitat use by the lungworm *Halocercus delphini* in the striped dolphin, *Stenella coeruleoalba*.

hemp cord and the furthest edge of the slice. This distance was divided to create, in the 3rd to 8th slices, three rings of equal thickness to represent the nuclear (N), intermediary (I), and peripheral (P) zones of the lung parenchyma surrounding the bronchus (Figure 1). Each of the 22 pieces of parenchyma was weighed on a scale (to the nearest 0.1 g) and had its volume measured (to the nearest ml) via water displacement in a 250 ml measuring cylinder. Each piece was then dissected individually in a Petri dish and analyzed for lungworms.

Kendall's concordance tests were used to assess the repeatability, from dolphin to dolphin, of patterns of worm number and density (per kilogram or liter) along the longitudinal axis (lung slices) or transversal axis (rings). The effects of increasing intensity on worm distribution along both axes was examined using (1) a mean location of worms as a measure of position (Moore & Simberloff, 1990) and (2) Levin's normalized niche breadth index as a measure of the worms' distribution spread (see, e.g., Simková et al., 2000). To calculate mean location in each lung, slices were numbered from 1 to 10 (cranial to caudal), and rings were named N, I, P (nuclear to peripheral), respectively; then, the slice or ring in which each worm was found was recorded. The mean location of colonization (i.e., the slice or ring in which a worm was most likely to be encountered) was then calculated as the mean of the weighted average location in each lung using the total number of worms in each section for the longitudinal and transversal axes.

Levin's normalized niche breadth (B_n) was calculated as:

$$B_n = 1/R \sum_i p_i^2$$

where p is the proportion of lungworms found in each unit i of a lung (i.e., slice or ring), and R is the number of units available. B_n varies from $1/R$ (all worms are concentrated in a single unit) to 1.0 (worms are equally distributed among units). Spearman's correlations were then used to test for monotonic trends of mean location and B_n at increasing overall lungworm intensity in the lung.

2.4 | Relationship between worm distribution and lung vascular system

We also investigated whether there was a positive relationship between worm distribution and the topology of the lung vascular system; we focused on the distribution of the segmental pulmonary arteries, which bring the blood from the heart to the lung tissues. To ascertain the distribution of these arteries, silicone casts of both the bronchial tree and the lung vascular system were obtained from a subadult striped dolphin from the Atlantic Center for Cetacean Research, University Institute of Animal Health and Food Safety (IUSA), University of Las Palmas de Gran Canaria, Las Palmas, Spain. The animal stranded alive and died one hour later, after which it was frozen to be necropsied later. During the necropsy, the cardiorespiratory system was removed and cleaned to remove blood clots. To obtain a cast of the bronchial tree, white silicon was pumped through the trachea with a 60 ml syringe, whereas liquid latex (300 ml) was used to obtain the cast of the blood vessels. Blue latex was pumped through the right atrium to fill the right ventricle, the pulmonary trunk, and the lung arteries; red latex was pumped through the left atrium to reach all the pulmonary veins. After 24 hr, the heart and lungs were submerged in 20% diluted sodium hydroxide and left for a week to remove the organic tissue. Further tissue remains were washed off with tap water.

Nakakuki's (1994) description of striped dolphin lungs was used to identify and name bronchioles in the cast, and to position each bronchiole with respect to each of the 10 longitudinal slices of the lung. The segmental arteries associated with each bronchiole were also visually counted in the cast, and their total number was considered as a proxy of the relative blood flow entering each lung slice.

We investigated whether the number of segmental arteries was a significant positive predictor of the number of worms found in each longitudinal slice via multilevel generalized linear mixed models (GLMM) based on the negative binomial distribution and a log link function. Following Singer's (1998) terminology, at level-2, "lung" (with two levels, left or right) and "host individual" ($n = 14$) were included in the fixed and random effects portions of the model,

respectively; at level-1, “no. arteries” and “slice mass” or “slice volume” (as a measure of space available for worm settlement) were included in the fixed effects portion, and “slice number” ($n = 10$) in the random effects portion. The interaction “lung \times no. arteries” was also included in the fixed effects portion to test for potential differences of regression slopes between the right and the left lung. Note that number of arteries and slice mass (or slice volume) were also initially included in the random effects portion of the models via an unstructured covariance structure (Singer, 1998). In this way, the intercepts and slopes of the regressions of the no. worms with the no. arteries or slice mass (or volume) were allowed to vary across host individuals (Singer, 1998). However, Akaike's information criterion (AIC) values (see below) increased enormously in this case and, therefore, the random effects of number of arteries and slice mass (or volume) were not further considered. All models were fitted using restricted maximum likelihood using a robust covariance structure; the degrees of freedom were calculated via the Satterthwaite approximation (Bolker et al., 2009).

GLMMs were also used to model the transversal distribution of *H. delphini* in the lung. In this case, the number of worms in the N, I, and P rings (regardless of longitudinal slice) was considered the dependent variable; at level-2, lung (with two levels, left or right) and host individual were included in the fixed and random effects portions of the model, respectively; at level-1, ring (with three levels ordered from inner to outer arrangement, i.e., 1 for N, 2 for I and 3 for P) and slice mass (or volume) in the fixed effects portion of the model; these predictors were also initially included in the random part of the model (see the previous paragraph) but were eventually not considered based on AIC analysis. The interaction “lung \times ring” was also included in the fixed effects portion of the models.

In the two GLMM analyses above, competing models with different numbers of predictors were compared based on values of Akaike's information criterion (AIC). The model with the lowest AIC for small sample sizes (AICc) was considered the best model, and the rest of the models were ranked according to increasing AICc values (Anderson & Burnham, 2004). Models with values of $\Delta\text{AICc} \leq 2$ with respect to the best model were considered to have substantial empirical support, whereas those with $\Delta\text{AICc} > 4$ were considered to have considerably less support (Anderson & Burnham, 2004) and will not be shown. Akaike weights (w_i) were calculated for models $\Delta\text{AICc} \leq 2$ according to Anderson and Burnham (2004).

2.5 | Microscale analysis

In a third sample of 18 dolphins, either the right or left lung was randomly selected and examined as described in Section 2.1; the other (10 left and 8 right) was used to obtain data on potential clusters of lungworms. In this case, the lungs were dissected by cutting along the airways from the bronchus to the caudal apex, but upon the discovery of a lungworm (hereafter a “focal lungworm”) the surrounding tissue was carefully cut and extracted to a radius approximately the same length as the visible caudal extremity of the focal lungworm. This radius allowed the focal lungworm to be maintained whole and also allowed the inclusion of neighboring lungworms that were close enough for reproduction to take place. Using a stereo microscope, the extracted tissue was dissected in a Petri dish with saline and all worms were identified and sexed. We attempted to find as many focal lungworms as possible in each lung, but due to the tendency of these lungworms to form knots in the parenchyma tissue, worms were fragile, and detection of intact worms was difficult. The rest of the lung tissue was carefully dissected, and all worms previously missed were then collected and counted.

To better interpret sex ratio composition of worm clusters, overall values of sex ratio for the whole lungworm population per host were obtained from a sample of 86 lungs (41 left and 45 right), each from a different dolphin. The sex ratio was calculated as the percentage of males present, and 95% CI for the average value per lung ($n = 86$) was set using the bootstrap method described in Section 2.1.

We explored whether the number of worms in the clusters around any focal worm increased with parasite intensity. To this end, we calculated the median number of worms per cluster for each dolphin and used linear regression

to test for a positive association with intensity. Potential changes of sex ratio in individual clusters with parasite intensity were investigated with a GAM as described in Section 2.2.

Quantitative Parasitology version 3.0 was used to calculate parasite burden parameters (Rózsa et al., 2000). All other statistical analyses were performed with SPSS version 26 (IBM Corp., Armonk, NY) or R (R Core Team, 2020). The significance level was set at $p < .05$.

3 | RESULTS

3.1 | Infection parameters

Of the 120 dolphins, 94 (78.3%, 95% CI [70.1–85.1]) were infected with a total of 6,653 specimens of *H. delphini*; mean abundance per dolphin was 55.4, 95% CI [40.9–76.3] and mean intensity 70.8, [52.5–94.0]. Individuals of another lungworm species, namely, *Stenurus ovatus*, were found in only 7 of the 120 dolphins (5.8%, thus their potential influence on the overall distribution patterns of *H. delphini* was considered negligible.

3.2 | Comparison of right versus left lung

As expected, the mass of the right and left lung differed significantly (mean [SD]: right lung 747.0 [248.0] vs. left lung 638.7 [113.7] g; paired $t = -2.70$, $df = 18$, one-tailed $p = .007$). The abundance of *H. delphini* was correspondingly higher in the right (mean 29.9, 95% CI [21.8–41.9]) vs. the left (25.6, [18.4–34.4]) lung, and the difference was highly significant (Wilcoxon's test $Z = 2.594$, $n = 94$, one-tailed $p = .002$). We failed to find a significant effect of intensity on percentage of worms in the right lung (GAM regression $\chi^2 = 0.783$, $edf = 1.004$, $p = .377$; Figure 2).

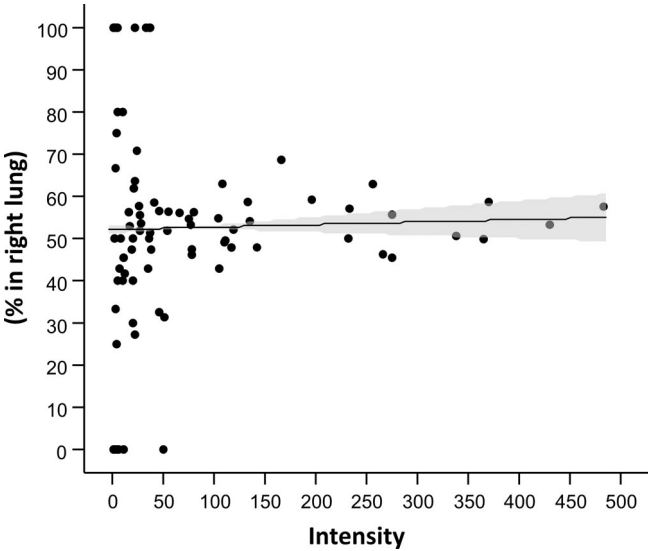


FIGURE 2 Percent of the total number of the nematode *Halocercus delphini* occurring in the right lung of 94 striped dolphins, *Stenella coeruleoalba*. The line and band represent predicted values and the 95% confidence interval, respectively, of the GAM-predicted smooth splines of sex ratio at increasing intensity.

3.3 | Worm distribution within the lung

Individuals of *H. delphini* were detected in all longitudinal lung slices, but their distribution was concentrated towards slices 4–9 (Table 1); this pattern was moderately repeatable (Kendall's concordance test, $W = 0.503$, 8 df , $p < .001$), but less so when considering worm density instead of number (density [mass], $W = 0.207$, $p = .002$; density [volume], $W = 0.200$, $p = .003$). At increasing intensity, worms' occurrence along the longitudinal axis exhibited a fairly nested pattern, i.e., at low intensity (<20), worms were largely concentrated in slices 4–9, whereas at higher intensities, they were spread along the whole longitudinal axis but still maintained a higher abundance in these slices (Table 2). This was confirmed by statistical analysis. First, the mean location (SD) of *H. delphini* along the longitudinal axis was 6.30 (0.67), i.e., between slices 6–7, and we found no statistical evidence that the mean location changed at increasing intensity (Spearman correlation, $r_s = -0.143$, $n = 14$, $p = .625$). In contrast, B increased significantly with intensity ($r_s = 0.683$, $n = 14$, $p = .007$).

Along the lung's transversal axis, the number of *H. delphini* appeared to decrease from the nuclear to the peripheral rings (Table 1), in a pattern that was fairly consistent from host to host ($W = 0.444$, $df = 2$, $p = .002$). However, repeatability dropped substantially when worm density, instead of number, was used (density [mass]: $W = 0.097$, $p = .257$; density [volume]: $W = 0.189$, $p = .071$). We did not find any significant relationship between intensity and mean location ($r_s = -0.125$, $n = 14$, $p = .671$) or B ($r_s = 0.058$, $n = 14$, $p = .857$).

3.4 | Relationship between worm distribution and lung vascular system

The cast of the bronchial tree and pulmonary vascular system allowed visualization of the main bronchioles and associated segmental arteries (Figure 3). The number of these arteries was more concentrated towards the caudal

TABLE 1 Features of distribution of the nematode *Halocercus delphini* in the lungs of striped dolphin, *Stenella coeruleaalba*. Shown are the mean mass and volume of each longitudinal subdivision (slice) and transversal subdivision (ring) of lungs (right or left pooled), along with the mean abundance, density per mass, and volume. In the case of the longitudinal axis, the number of segmental arteries for the right (R) and left (L) lung arising in each slice are also provided (see also Figure 3).

Slice	Mass (g)		Volume (ml)		No. arteries			Abundance		Density (worms/kg)		Density (worms/L)	
	Mean	SD	Mean	SD	R	L	Total	Mean	SD	Mean	SD	Mean	SD
1	24.7	23.3	27.4	24.4	0	0	0	0.6	1.1	34.5	53.9	22.4	53.7
2	40.4	25.7	50.1	34.1	2	0	2	1.1	1.6	30.2	42.6	21.1	34.5
3	61.0	30.5	70.1	31.7	0	4	4	1.7	2.0	24.8	27.6	16.6	24.7
4	90.5	44.4	105.7	49.2	4	5	9	3.4	3.5	40.5	50.4	32.1	51.4
5	109.8	45.8	130.1	52.7	9	4	13	3.1	2.2	29.0	22.0	20.0	18.8
6	123.8	42.3	145.4	49.5	8	7	15	7.3	5.1	64.4	46.9	47.7	39.9
7	113.6	34.8	128.7	39.0	4	6	10	4.9	2.9	47.6	33.6	33.4	28.3
8	79.5	31.3	91.5	31.2	7	6	13	5.4	6.0	67.2	64.5	53.3	79.4
9	45.3	20.3	51.4	20.4	2	6	8	3.4	2.3	81.2	58.1	58.7	52.1
10	16.5	11.4	17.7	9.4	0	0	0	0.7	0.9	46.1	69.0	30.8	51.0
Ring													
N	165.5	53.0	186.5	47.5				12.1	11.9	79.4	75.8	68.2	65.8
I	255.8	104.9	293.1	110.4				10.7	5.6	42.0	17.7	35.7	13.4
P	141.1	60.6	171.1	83.6				4.6	3.9	32.7	26.3	26.6	20.7

TABLE 2 Number of *Halocercus delphini* in each of 10 longitudinal lung slices of 14 striped dolphins, *Stenella coeruleoalba*. Dolphins have been arranged according to the total number of worms, and cells with more worms have been colored darker (color categories: 1–5, 5–7, 8–14, 15–20 worms). Note that a single lung, left (L) or right (R) is analyzed for each dolphin.

Slice	Dolphin													
	1	2	3	4	5	6	7	8	9	10	11	12	13	14
1	0	0	0	0	0	1	1	0	1	0	4	1	1	0
2	0	0	0	0	2	3	0	0	1	1	5	1	0	3
3	0	0	0	0	0	2	3	2	3	2	3	2	0	7
4	0	0	1	2	1	2	2	5	1	2	8	3	9	11
5	0	3	1	0	2	4	3	2	2	6	5	4	3	8
6	6	1	0	3	7	7	4	6	9	12	5	15	9	18
7	0	2	1	6	4	7	7	9	1	8	5	6	7	5
8	0	1	2	0	2	1	6	3	9	5	6	4	17	19
9	1	0	3	4	1	1	3	3	6	6	2	6	5	7
10	0	0	1	1	0	0	1	2	1	0	0	1	0	3
Total	7	7	9	16	19	28	30	32	34	42	43	43	51	81

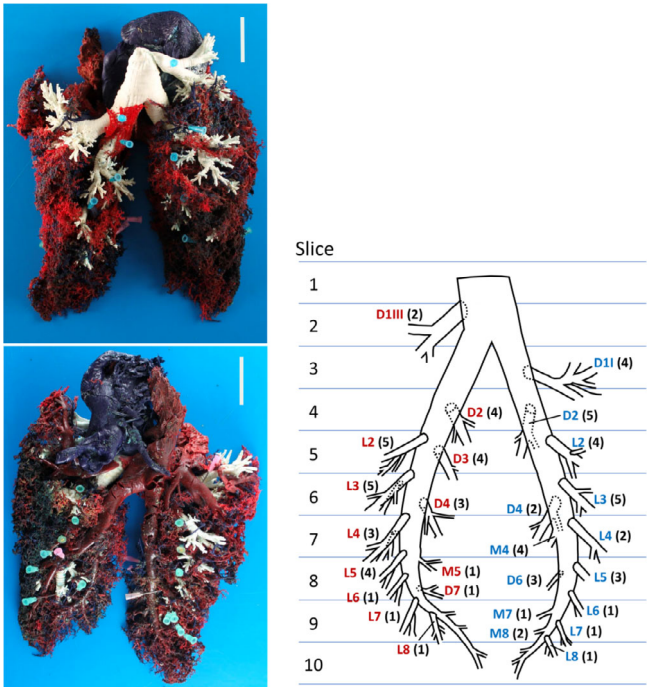


FIGURE 3 Pulmonary vascular system of the striped dolphin, *Stenella coeruleoalba*. Pictures on the left show a dorsal (above) and ventral (below) view of a cast of the bronchial tree (in white), and the associated arterial (in blue) and venous (in red) system; the right side of the heart is also present. Needles are used to indicate the branching of airways. Scale bar: 5 cm. Photo credit: IUSA - ULPGC (Consoli, 2016). On the right, a simplified scheme of Nakakukis's (1994) bronchial tree (abbreviate) nomenclature is shown (red: right lung; blue: left lung), along with the approximate placement of the 10-slice longitudinal subdivision used in the present study (see the text for details). The number of segmental arteries associated with each bronchiole is shown parentheses.

TABLE 3 Competing generalized linear mixed models that account for the number of *Halocercus delphini* in 10 slices of equal thickness along the lung's longitudinal axis (see Figure 1) obtained from 14 western Mediterranean striped dolphins, *Stenella coeruleoalba*. Models are ordered according to the Akaike's Information Criterion (AIC); those with $\Delta\text{AIC} > 4$ with respect to the best model are not shown. Akaike weights (w_i) for the selected models are also provided. "Lung" indicates whether the lung was left or right, and the parameter value is that of the left lung after setting that of the right one to zero; 'No. arteries' stands for the number of segmental arteries associated with each slice. (See the text for details).

Model	ΔAIC	w_i	Predictor	Parameter [95% CI]	F	g1. g2	p
No. arteries + Slice volume + Lung	0	0.243	No. arteries	0.105 [0.019, 0.190]	5.90	1. 111	.017
			Slice volume	0.008 [0.003, 0.013]	10.01	1. 87	.001
			Lung	−0.600 [−1.329, 0.129]	3.30	1. 11	.097
No. arteries + Slice mass + Lung	0.071	0.234	No. arteries	0.102 [0.013, 0.191]	5.18	1. 111	.025
			Slice volume	0.008 [0.003, 0.013]	9.52	1. 74	.003
			Lung	−0.600 [−1.329, 0.129]	1.71	1. 11	.217
No. arteries + Slice mass + Lung + No. arteries*Lung	0.667	0.174	No. arteries	0.093 [0.020, 0.174]	8.19	1. 83	.005
			Slice mass	0.009 [0.003, 0.015]	10.13	1. 57	.002
			Lung	−0.920 [−1.900, 0.061]	3.61	1. 38	.065
			No. arteries*Lung	0.098 [−0.041, 0.237]	1.94	1. 135	.237
No. arteries + Lung	1.167	0.136	No. arteries	0.174 [0.089, 0.258]	19.14	1. 15	<.001
			Lung	−0.662 [−1.474, 0.150]	3.22	1. 11	.100
No. arteries + Lung + No. arteries*Lung	1.467	0.117	No. arteries	0.166 [0.085, 0.248]	30.58	1. 13	<.001
			Lung	−1.122 [−2.130, −0.113]	5.10	1. 35	.030
			No. arteries*Lung	0.100 [−0.042, 0.241]	1.93	1. 136	.167
No. arteries + Slice Volume + Lung + No. arteries*Lung	1.849	0.096	No. arteries	0.095 [0.007, 0.182]	7.42	1. 88	.008
			Slice mass	0.008 [0.003, 0.012]	10.63	1. 71	.002
			Lung	−0.894 [−1.842, 0.054]	3.62	1. 38	.064
			No. arteries*Lung	0.063 [−0.077, 0.207]	0.80	1. 135	.374

TABLE 4 Competing generalized linear mixed models that account for the distribution of *Halocercus delphini* in 14 western Mediterranean striped dolphins, *Stenella coeruleoalba*, along the transversal axis of the lung. Models are ordered according to the Akaike's information criterion (AIC); those with $\Delta\text{AIC} > 4$ with respect to the best model are not shown. Akaike weights (w_i) for the selected models are also provided. Data were obtained by dividing individual lungs per dolphin (seven right and seven left) into 10 slices of equal thickness along the lung's longitudinal axis (see Figure 1). Slices 3 to 8 were further subdivided into three rings of equal width, i.e., inner, intermediate, and outer (see Figure 1), and the number of *H. delphini* in each ring were summed up for the six slices. "Lung" indicates whether the lung was left or right, and the parameter value is that of the left lung after setting that of the right one to zero.

Model	ΔAIC	w_i	Predictor	Parameter [95% CI]	F	g1. g2	p
Ring + Lung	0	0.516	Ring	−0.447 [−0.740, −0.154]	9.54	1. 39	.004
			Lung	−0.561 [−1.262, 0.141]	3.05	1. 12	.108
Ring + Lung + Ring*Lung	0.784	0.349	Ring	−0.523 [−0.920, −0.126]	1. 38	9.31	.004
			Lung	−0.896 [−2.183, 0.390]	1. 38	1.99	.166
			Ring*Lung	0.173 [−0.406, 0.753]	1. 38	0.37	.549
Ring	2.676	0.135	Ring	−0.456 [−0.767, −0.146]	8.83	1. 40	.006

section of the lung, especially in the right lung, in the 4th to 9th slices (Figure 3, Table 1). There was a strong correlation between the number of segmental arteries and the lung mass (Spearman correlation, $r_s = 0.915$, $n = 10$, $p < .001$) or volume ($r_s = 0.915$, $n = 10$, $p < .001$) of slices (Table 1).

Along the longitudinal axis, the number and density of *H. delphini* was higher in larger slices containing more segmental arteries (Table 1). The GLMM did indeed reveal a specific effect of the number of segmental arteries on the number of worms per slice (Table 3). All the five competing models with $\Delta\text{AICc} \leq 2$ included a positive effect of "no. segmental arteries"; furthermore, from a frequentist perspective, this predictor was also statistically significant in all selected models (Table 3). As may be expected, slice mass or volume had positive effects on the number of *H. delphini*, and the right lung had more worms than the left (Table 3).

Only three competing models with $\Delta\text{AICc} \leq 2$ accounted for the distribution of *H. delphini* along the transversal axis of the lung, and all of them included "ring" as a negative, significant predictor (Table 4). This therefore indicated that the number of worms decreased towards the lung periphery regardless of ring mass or volume, or whether the lung is right or left. Also note that "lung," but not "ring mass" and "ring volume," were included in all of the models with $\Delta\text{AICc} \leq 2$.

3.5 | Microscale

A total of 194 worms could be found in 11 of the 18 lungs analyzed, with a total of 55 focal worms in the overall sample and a range from 1 to 13 per dolphin (Figure 4a). Solitary focal worms were found in 13 cases (23.6%); clusters with 2–4 worms in 30 cases (54.6%), and clusters with >4 worms in 12 cases (21.8%) (Figure 4a). Interestingly, even in lungs harboring <10 worms, solitary focal worms were less frequent than those occurring in clusters (5 vs. 6 with >4 worms in 12 cases (21.8%; Figure 4a). Furthermore, there was a strong, linear relationship between the median number of worms in the cluster and the intensity of infection (linear regression, slope = 0.052, 95% CI [0.035–0.069], $r^2 = 0.837$, $F_{(1, 10)} = 46.20$, $p < 0.001$; Figure 4b).

Mean overall sex ratio per lung was strongly biased against males (33.1%, 95% CI [28.9–37.7]). The GAM regression of intensity on sex ratio was highly significant ($\chi^2 = 19.61$, $\text{edf} = 3.526$, $p = .00103$), although the deviance explained was low (5.7%). The trend indicates that the bias against males was stronger at intensities ≤ 20 worms, then

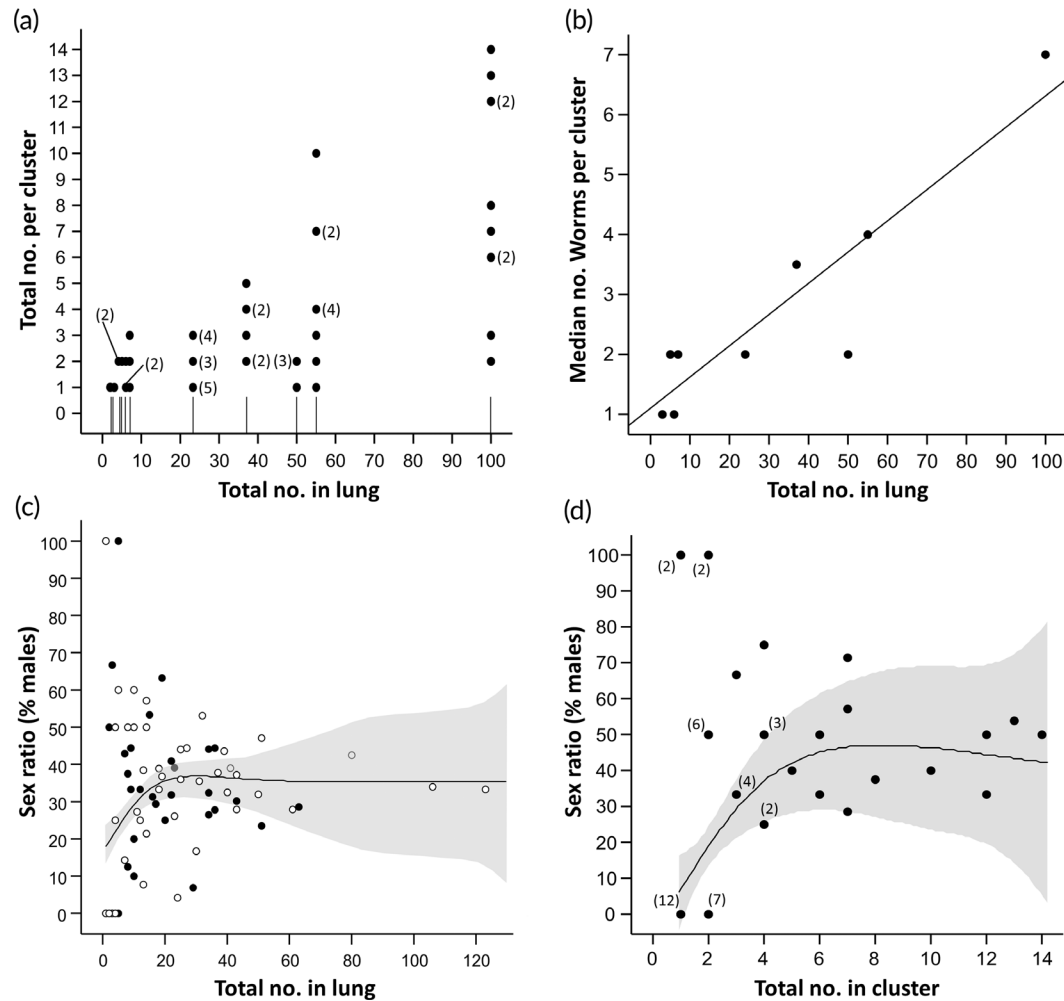


FIGURE 4 Distribution and sex ratio of the nematode *Halocercus delphini* around selected worms (focal worms) in the lung (right or left) of 11 striped dolphins, *Stenella coeruleoalba* (see the text for details); (a) Number of individuals per cluster at increasing intensity; (b) Median number of worms in clusters per dolphin at increasing intensity; (c) Sex ratio (percent males) at increasing intensity in 86 lungs, 41 left (black dots) and 45 right (empty dots) from different dolphins; (d) Sex ratio per cluster at increasing number of worms in the cluster. Numbers in parentheses indicate the number of cases represented by the dot when $n > 1$. In (b), the line represents the linear regression; in (c) and (d), the lines and bands represent predicted values and the 95% confidence interval, respectively, of the GAM-predicted smooth splines.

stabilized (Figure 4c). In only 9 of the 86 dolphins the sex ratio favored males; in all cases the intensity was <20 worms, and in 6 it was ≤ 10 worms. The mean sex ratio found in worm clusters paralleled that of the overall worm population per host, i.e., 35.8% (27.4%–44.4%); note that 6 of the 194 worms (3.1%) could not be sexed. Similar to the overall sex ratio, the bias against males was stronger at lower number of worms (<3 worms) around the focal worm (GAM regression, $\chi^2 = 13.02$, $edf = 2.272$, $p = .00668$) (Figure 4d).

4 | DISCUSSION

Our results indicate a clear positive relationship between the number of *H. delphini* and the amount of blood perfusion in the lungs. First, the parasite burden was slightly, but significantly, higher in the right lung, which was also

significantly larger than the left lung. This difference could be explained by the obvious association between organ size and degree of perfusion, which could result, at least in part, from the fact that the right lung of striped dolphins possesses a *bronchus trachealis* (Nakakuki, 1994), similar to other cetaceans (Kida, 1998). It is perhaps not coincidental that the region where the *bronchus trachealis* extends into the right lung (1st–3rd slices) was found to be more frequently infected (6 out of 7 cases, vs. 4 out of 7 in the left lung). Unfortunately, the lung sample size ($n = 14$) was too small to perform a specific test in contrast with the overall comparison between lungs ($n = 120$).

Second, and more instructively, there was a significant positive relationship between the number of worms per lung slice and the number of segmental arteries entering each of them regardless of slice size or whether the lung was left or right. Worms were readily spread along the longitudinal axis of the lung even at low intensities, but tended to be concentrated in slices with more arteries. Admittedly, some of these arteries traverse several slices, but the arteries are all concentrated in the lung region with the highest observed density of *H. delphini*,

In summary, individuals of *H. delphini* would end up in a specific lung, or a specific slice within the lung, depending primarily on the number and size of arteries entering each site from the pulmonary artery. This hypothesis is also supported by the patterns of colonization at increasing intensity. On the one hand, the relative number of worms colonizing the right lung was unaffected by infrapopulation size; on the other, the occupation of the lung along its longitudinal axis followed a nested pattern, with worms sequentially spreading, at higher intensities, without a change in the mean location of worms. Both patterns are easily explained if we consider different colonization probabilities between lungs, or slices, according to their degree of perfusion. And, because this process is not deterministic, just a low to moderate repeatability of colonization patterns would be expected, as we did indeed observe.

The metastrongyloid nematodes that are more closely related to the Pseudaliidae infect the lungs of carnivores (Pool et al., 2023) and have developed different migration routes to reach this organ (Anderson, 2000). In *Aelurostrongylus abstrusus* (from cats) and *A. priidhami* (from minks), the ingested larvae penetrate the gastric wall, cross the peritoneal cavity, pass through the diaphragm into the thoracic cavity, and move into the lung parenchyma by penetrating the visceral pleura (Stockdale, 1970). In contrast, larvae of *Filaroides martis* (in minks) migrate via the adventitia of the arteries from the stomach wall to the lung (Stockdale & Anderson, 1970), whereas larvae of *Crenosoma vulpis* penetrate the intestine and enter the hepatic portal vein where they are carried by the bloodstream to the heart and then finally to the lungs via the pulmonary circulatory system (Stockdale & Hullah, 1970). Data from the present study conform to the latter two possibilities, i.e., *H. delphini* would use the circulatory system (the arterial adventitia or, perhaps most likely, the bloodstream), rather than direct penetration of the pleura, to reach the lungs.

The transversal distribution of the *H. delphini* in the lung decreased monotonically from the areas closer to the bronchi to the peripheral parenchyma associated with lesser bronchioles, even though the intermediate ring of tissue was the largest of the three transversal subdivisions. While this distribution could be attributed to the well-perfused nature of the major airways (see above), it could also be an indication of a strategy by the mating worms to maximize the diffusion of larvae to the environment and minimize the distance to the exit route. It should be emphasized that, regardless of the release path, i.e., feces, or sputum (see below), the larvae lungworms infecting terrestrial mammals invariably leave the lung via the bronchial escalator (Anderson, 2000; Cowie, 2013; Georgi et al., 1979).

The fine-scale distribution of *H. delphini* indicates that worms frequently cluster together; pairs, or even trios, of individuals of both sexes were found at very low intensities ($n < 10$ worms). This strongly suggests that these worms have ability to find, or at least detect, one another even at low population density. In fact, there is solid evidence that chemical signaling through pheromones is common in mate-seeking nematodes (e.g., Choe et al., 2012; MacKinnon, 1987). Moreover, Erdongan et al. (2021) recently described a “follow the leader” effect in entomopathogenic nematodes, where conspecifics followed the trail of one another if the lead nematode had first contacted the host tissue. Accordingly, it may be not surprising that the median number of *H. delphini* increased in the clusters at higher overall intensity (assuming no repulsion responses, see, e.g., Bone & Shorey, 1977). However, pheromone gradients operate at short distances, i.e., centimeters (see, e.g., Bone & Shorey, 1977; García-Rejón

et al., 1985), thus raising the question of how aggregations of *H. delphini* can be formed even in apparently sparse infrapopulations.

The overall sex ratio in *H. delphini* aggregates was strongly female-biased, more so when the number of individuals was very small; in fact, solitary worms were much more frequently females; these patterns mirrored those obtained for the overall infrapopulation. Female-biased sex ratios are commonly observed in parasitic nematodes and have been accounted for by two phenomena (Poulin, 1997). It may be that females just have a longer lifespan (for pseudaliids, see Measures, 2001). However, a female-biased sex ratio could also be adaptive; based on theoretical grounds, it maximizes the mean number of mated females per host when the mating system is polygamous and the parasite distribution among hosts is aggregated (May & Woolhouse, 1978; Van Goor et al., 2022).

Similar to other pseudaliid species, *H. delphini* is ovoviviparous and so an interesting question is how the larvae shed by females reach the exterior environment. In the vast majority of their terrestrial metastrongyloid counterparts, larvae climb the bronchial escalator, are coughed up, swallowed, and released with feces (Anderson, 2000). In agreement with this, there is a report of larvae of *Halocercus lagenorhynchi* in the feces of bottlenose dolphins, *Tursiops truncatus*, although with low prevalence (Fauquier et al., 2009). In contrast, records of *Halocercus* spp. in the blowhole of dolphins are frequent (Caldwell et al., 1968; Fauquier et al., 2009; Woodard, 1968), raising the question over the relative importance of each pathway for the release of lungworm larvae. Cetaceans are peculiar in that their respiratory system is largely isolated from the digestive system. Their larynx extends through the esophagus into the nasal passage and is sealed into place by the palatopharyngeal sphincter muscle, which allows food to pass on either side of the larynx (Bueno Mariani et al., 2020; Reidenberg & Laitman, 1987). It is still possible that lungworm larvae can reach the gut as in terrestrial metastrongyloids, but this pathway is not expected to be easy to follow. Whether the pseudaliid larvae preferentially use the blowhole to exit the host is an open question but, to our knowledge, this mechanism would represent a strategy unique to the Pseudaliidae, and was likely developed as an adaptation to overcome the unique physiology of cetaceans.

In summary, we believe that this study delivers convincing evidence that the large-scale distribution of *H. delphini* is related to the perfusion of the lung, with small-scale aggregations likely resulting from an active reproductive behavior of the worms. Incidentally, the evidence of migration of *H. delphini* larvae via the circulatory system does provide support to the hypothesis of transplacental transmission (Caldwell et al., 1968; Dailey et al., 1991; Fauquier et al., 2009). The ability of the Pseudaliidae to be transmitted both horizontally and vertically raises the possibility of direct and indirect life cycles. This has been demonstrated to limited effect in the terrestrial metastrongyloid species *Andersonstrongylus captivensis* (Angiostrongylidae), *Filaroides hirthi*, and *Oslerus osleri* (Filaroididae), which all infect their hosts as first-stage larvae (Anderson, 2000).

Furthermore, the present investigation highlights areas for future research, including the examination of blood vessels for pseudaliid larvae, and the identification of the exact pathway to the lungs from the digestive system, which could also shed light on the route taken by larvae during vertical transmission, transplacentally (Fauquier et al., 2009; Pool, Chandradeva, et al., 2020; Reckendorf et al., 2018). Additional efforts should also be made in attempting to quantify the relative contributions of each mechanism of transmission, i.e., aerosol, trophic, and transplacental.

ACKNOWLEDGMENTS

We greatly appreciate the assistance of our colleagues from the Marine Zoology Unit, University of Valencia with stranded dolphins. We also thank Francesco Consoli and Miguel Rivero from the Atlantic Center for Cetacean Research, University Institute of Animal Health and Food Safety (IUSA), University of Las Palmas de Gran Canaria, and Cristiano Bombardi from Almamater Studiorum Bologna, for sharing with us the details and findings of their experiments with the silicone and latex lung molds. This work was supported by the projects AICO/

2021/022, from the Conselleria de Educació, Universidades y Empleo, Generalitat Valenciana and VARACOMVAL, from the Biodiversity Foundation, MITECO.

AUTHOR CONTRIBUTIONS

Rachel V. Pool: Conceptualization; data curation; formal analysis; investigation; methodology; visualization; writing – original draft; writing – review and editing. **Neus Pons-García:** Data curation; investigation; methodology; writing – original draft. **Francesco Consoli:** Methodology; visualization; writing – review and editing. **Miguel Rivero:** Methodology; resources; visualization; writing – review and editing. **Cristiano Bombardi:** Methodology; resources; writing – review and editing. **Juan A. Raga:** Funding acquisition; project administration; resources; supervision; writing – review and editing. **Francisco J. Aznar:** Conceptualization; data curation; formal analysis; funding acquisition; investigation; methodology; project administration; resources; software; supervision; validation; visualization; writing – original draft; writing – review and editing.

ORCID

Rachel V. Pool  <https://orcid.org/0000-0001-9594-102X>

Francisco J. Aznar  <https://orcid.org/0000-0002-1316-1175>

REFERENCES

- Anderson, R. C. (2000). Strongylida: Metastrongyloidea. In R. C. Anderson (Ed.), *Nematode parasites of vertebrates: their development and transmission* (2nd ed., pp.178–217. CAB International. <https://doi.org/10.1079/9780851994215.0041>
- Anderson, R. C. (2009). Strongylida: Metastrongyloidea. In R. C. Anderson, A. G. Chabaud, & S. Willmott (Eds.), *Keys to the nematode parasites of vertebrates*. (pp.178–217). CAB International. <https://doi.org/10.1079/9781845935726.0178>
- Aznar, F. J., Fognani, F. J., Balbuena, J. A., Pietrobelli, M. & Raga, J. A. (2006). Distribution of *Pholeter gastrophilus* (Digenea) within the stomach of four odontocete species: the role of the diet and digestive physiology of hosts. *Parasitology*, 133, 369–380. <https://doi.org/10.1017/S0031182006000321>
- Baylis, H. A., & Daubney, R. (1925). A revision of the lungworms of Cetacea. *Parasitology*, 17(2), 201–216. <https://doi.org/10.1017/S0031182000004595>
- Bolker, B. M., Brooks, M. E., Clark, C. J., Geang, S. W., Poulsen, J. R., Stevens, M. H. H., & White, J. S. S. (2009). Generalized linear mixed models: a practical guide for ecology and evolution. *Trends in Ecology & Evolution*, 24, 127–135. <https://doi.org/10.1016/j.tree.2008.10.008>
- Bone, L., & Shorey, H. H. (1977). Interactive influences of male- and female-produced pheromones on male attraction to female *Nippostrongylus brasiliensis*. *Journal of Parasitology*, 63(5), 845–848. <https://doi.org/10.2307/3279890>
- Brosens, L., Jauniaux, T., Siebert, U., Benke, H., & Coignoul, F. (1996). Observations on the helminths of harbour porpoises (*Phocoena phocoena*) and common guillemots (*Uria aalge*) from the Belgian and German coasts. *Veterinary Record*, 139(11), 254–257. <https://doi.org/10.1136/vr.139.11.254>
- Bueno Mariani, D., Plácido Guimarães, J., Guedes Batista, R., Brum, A., Groch, K. R., Díaz-Delgado, J., & Vergara Parente, J. E. (2020). Fatal asphyxia due to laryngeal displacement by large-sized prey in a Guiana dolphin (*Sotalia guianensis*), Brazil. *Ciência Rural*, 50(2), Article e20190068. <https://doi.org/10.1590/0103-8478cr20190068>
- Burek-Huntington, K. A., Dushane, J. L., Goertz, C. E., Romero, C. H., Raverty, S. A. (2015). Morbidity and mortality in stranded Cook Inlet beluga whales *Delphinapterus leucas*. *Diseases of Aquatic Organisms*, 114(1), 45–60. <https://doi.org/10.3354/dao02839>
- Burnham, K. P., & Anderson, D. R. (Eds.). (2004). Basic use of the information – theoretic approach. *Model selection and multi-model inference* (pp. 98–148). Springer. https://doi.org/10.1007/978-0-387-22456-5_3
- Bush, A. O., Lafferty, K. D., Lotz, J. M., & Shostak, A. W. (1997). Parasitology meets ecology on its own terms: Margolis et al. revisited. *Journal of Parasitology*, 83(4), 575–583. <https://doi.org/10.2307/3284227>
- Caldwell, M. C., Caldwell, D. K., & Zam, S. G. (1968). Occurrence of the lungworm (*Halocercus* sp.) in Atlantic bottlenose dolphins (*Tursiops truncatus*) as a husbandry problem. In D. K. Caldwell & M. C. Caldwell (Eds.), *Proceedings of the Second Symposium on Diseases and Husbandry of Aquatic Mammals* (pp. 11–15). Marineland of Florida, St. Augustine, Florida.
- Choe, A., Chuman, T., von Reuss, S. H., Dossey, A. T., Yim, J. J., Ajredini, R., Kolawa, A. A., Kaplan, F., Alborn, H. T., Teal, P. E., & Schroeder, F. C. (2012). Sex-specific mating pheromones in the nematode *Panagrellus redivivus*. *Proceedings of the National Academy of Sciences of the United States of America*, 109(51), 20949–20954. <https://doi.org/10.1073/pnas.1218302109>

- Consoli, F. (2016). *Caratteristiche morfologiche e strutturali dei vasi sanguiferi polmonari presenti nella Stenella striata* (Stenella coeruleoalba) [Morphological and structural characteristics of the pulmonary blood vessels present in the striped dolphin (Stenella coeruleoalba)] [Trabajo de tesis de laurea]. Università di Bologna.
- Cowie, R. H. (2013). Biology, systematics, life cycle, and distribution of *Angiostrongylus cantonensis*, the cause of rat lung-worm disease. *Hawai'i Journal of Medicine & Public Health*, 72(6 Suppl 2), 6–9.
- Dailey, M., Walsh, M., Odell, D., & Campbell, T. (1991). Evidence of prenatal infection in the bottlenose dolphin (*Tursiops truncatus*) with the lungworm *Halocercus lagenorhynchi* (Nematoda: Pseudaliidae). *Journal of Wildlife Diseases*, 27(1), 164–165. <https://doi.org/10.7589/0090-3558-27.1.164>
- Erdogan, H., Cruzado-Gutierrez, K., Stevens, G., Shapiro-Ilan, D., Kaplan, F., Alborno, H., & Lewis, E. (2021). Nematodes follow a leader. *Frontiers in Ecology and Evolution*, 9, Article 740351. <https://doi.org/10.3389/fevo.2021.740351>
- Fauquier, D. A., Kinsel, M. J., Dailey, M. D., Sutton, G. E., Stolen, M. K., Wells, R. S., & Gulland, F. M. D. (2009). Prevalence and pathology of lungworm infection in bottlenose dolphins *Tursiops truncatus* from southwest Florida. *Diseases of Aquatic Organisms*, 88, 85–90. <https://doi.org/10.3354/dao02095>
- Fraija-Fernández, N., Fernández, M., Raga, J. A., & Aznar, F. J. (2016). Helminth diversity of cetaceans: An update. In A. Kovacs & P. Nagy (Eds.), *Advances in marine biology* (pp. 29–100). Nova Science Publishers.
- Gallego, J., & Selva, J. M. (1979). *Skrjabinalius guevarai* n. sp. (Nematoda: Pseudaliidae), parasito pulmonar del delfin mular, *Tursiops truncatus* Montagu, 1821 (Cetacea: Delphinidae) en el Adriatico [*Skrjabinalius guevarai* n. sp. (Nematoda: Pseudaliidae), pulmonary parasite of the bottlenose dolphin, *Tursiops truncatus* Montagu, 1821 (Cetacea: Delphinidae) in the Adriatic]. *Revista Iberica de Parasitologia*, 39, 203–208.
- García-Rejon, L., Verdejo, S., Sanchez-Moreno, M., & Monteoliva, M. (1985). Some factors affecting sexual attraction in *Ascaris suum* (Nematoda). *Canadian Journal of Zoology*, 63(9), 2074–2076. <https://doi.org/10.1139/z85-304>
- Geraci, J. R. (1979). The role of parasites in marine mammal strandings along the New England coast. In J. R. Geraci & D. J. St. Aubin (Eds.), *Biology of marine mammals: Insights through strandings* (NTIS Report PB-293-890; pp. 85–91). U.S. Department of Commerce.
- Geraci, J. R., & Lounsbury, V. J. (2005). *Marine mammals ashore: A field guide for strandings*. National Aquarium in Baltimore.
- Georgi, J. R., Fahnestock, G. R., Bohm, M. F., & Adsit, J. C. (1979). The migration and development of *Filaroides hirthi* larvae in dogs. *Parasitology*, 79(1), 39–47. <https://doi.org/10.1017/S0031182000051969>
- Holmes, J. C. (1990). Competition, contacts, and other factors restricting niches of parasitic helminths. *Annales de Parasitologie Humaine et Comparée*, 65, 69–72. <https://doi.org/10.1051/parasite/1990651069>
- Kida, M. Y. (1998). Morphology of the tracheobronchial tree and the route of the pulmonary artery in the fetal minke whale (*Balaenoptera acutorostrata*). *Okajimas folia anatomica Japonica*, 75(5), 251–258. https://doi.org/10.2535/ofaj1936.75.5_251
- Lymbery, A. J., Hobbs, R. P., & Thompson, R. C. A. (1989). The dispersion of *Echinococcus granulosus* in the intestine of dogs. *Journal of Parasitology*, 75(4), 562–570. <https://doi.org/10.2307/3282907>
- MacKinnon, B. M. (1987). Sex attractants in nematodes. *Parasitology Today*, 3, 156–158. [https://doi.org/10.1016/0169-4758\(87\)90201-8](https://doi.org/10.1016/0169-4758(87)90201-8)
- Mateu, P., Raga, J. A., Fernández, M., & Aznar, F. J. (2014). Intestinal helminth fauna of striped dolphins (*Stenella coeruleoalba*) in the western Mediterranean: No effects of host body length, age and sex. *Marine Mammal Science*, 30(3), 961–977. <https://doi.org/10.1111/mms.12096>
- May, R. M., & Woolhouse, M. E. J. (1993). Biased sex ratios and parasite mating probabilities. *Parasitology*, 107, 287–295. <https://doi.org/10.1017/S0031182000079269>
- Measures, L. N. (2001). Lungworms of marine mammals. In W. Samuel, M. Pybus, & A. Kocan (Eds.), *Parasitic diseases of wild mammals* (pp. 279–300). Iowa State Press. <https://doi.org/10.1002/9780470377000.ch10>
- Moore, J., & Simberloff, D. (1990). Gastrointestinal helminth communities of bobwhite quail. *Ecology*, 71, 344–59. <https://doi.org/10.2307/1940273>
- Nakakuki, S. (1994). The bronchial tree and lobular division of the lung in the striped dolphin (*Stenella coeruleoalba*). *Journal of Veterinary Medical Science*, 56(6), 1209–1211. <https://doi.org/10.1292/jvms.56.1209>
- Piscitelli, M. A., Raverty, S. A., Lillie, M. A., & Shadwick, R. E. (2013). A review of cetacean lung morphology and mechanics. *Journal of Morphology*, 274(12), 1425–1440. <https://doi.org/10.1002/jmor.20192>
- Pool, R., Chandradeva, N., Gkafas, G., Raga, J. A., Fernández, M., & Aznar, F. J. (2020). Transmission and predictors of burden of lungworms of the striped dolphin (*Stenella coeruleoalba*) in the Western Mediterranean. *Journal of Wildlife Diseases*, 56(1), 186–191. <https://doi.org/10.7589/2018-10-242>
- Pool, R., Fernández, M., Chandradeva, N., Raga, J. A., & Aznar, F. J. (2020). The taxonomic status of *Skrjabinalius guevarai* Gallego & Selva, 1979 (Nematoda: Pseudaliidae) and the synonymy of *Skrjabinalius* Delyamure, 1942 and *Halocercus* Baylis & Daubney, 1925. *Systematic Parasitology*, 97, 389–401. <https://doi.org/10.1007/s11230-020-09921-9>
- Pool, R., Shiozaki, A., Raga, J. A., Fernández, M., & Aznar, F. J. (2023). Molecular phylogeny of the Pseudaliidae (Nematoda) and the origin of associations between lungworms and marine mammals. *International Journal for Parasitology: Parasites and Wildlife*, 20, 192–202. <https://doi.org/10.1016/j.ijppaw.2023.03.002>

- Poulin, R. (1997). Population abundance and sex ratio in dioecious helminth parasites. *Oecologia*, 111(3), 375–380. <https://doi.org/10.1007/s004420050248>
- R Core Team. (2020). *R: A language and environment for statistical computing* [Computer software]. R Foundation for Statistical Computing.
- Reckendorf, A., Ludes-Wehrmeister, E., Wohlsein, P., Tiedemann, R., Siebert, U., & Lehnert, K. (2018). First record of *Halocercus* sp. (Pseudaliidae) lungworm infections in two stranded neonatal orcas (*Orcinus orca*). *Parasitology*, 145(12), 1553–1557. <https://doi.org/10.1017/s0031182018000586>
- Reiczgel, J., Marozzi, M., Fábán, I., & Rózsa, L. (2019). Biostatistics for parasitologists—a primer to quantitative parasitology. *Trends in Parasitology*, 35(4), 277–281. <https://doi.org/10.1016/j.pt.2019.01.003>
- Reidenberg, J. S., & Laitman, J. T. (1987). Position of the larynx in Odontoceti (toothed whales). *Anatomical Record*, 218(1), 98–106. <https://doi.org/10.1002/ar.1092180115>
- Rohde, K. (1994). Niche restriction in parasites: proximate and ultimate causes. *Parasitology*, 109(S1), S69–S84. <https://doi.org/10.1017/s0031182000085097>
- Rózsa, L., Reiczgel, J., & Majoros, G. (2000). Quantifying parasites in samples of hosts. *Journal of Parasitology*, 86(2), 228–232. [https://doi.org/10.1645/0022-3395\(2000\)086\[0228:qpiroh\]2.0.co;2](https://doi.org/10.1645/0022-3395(2000)086[0228:qpiroh]2.0.co;2)
- Siebert, U., Wünschmann, A., Weiss, R., Frank, H., Benke, H., & Frese, K. (2001). Post-mortem findings in harbour porpoises (*Phocoena phocoena*) from the German North and Baltic Seas. *Journal of Comparative Pathology*, 124(2–3), 102–114. <https://doi.org/10.1053/jcpa.2000.0436>
- Simková, A., Desdevises, Y., Gelnar, M., & Morand, S. (2000). Co-existence of nine gill ectoparasites (*Dactylogyrus*: Monogenea) parasitising the roach (*Rutilus rutilus* L.): history and present ecology. *International Journal for Parasitology*, 30, 1077–1088. [https://doi.org/10.1016/s0020-7519\(00\)00098-9](https://doi.org/10.1016/s0020-7519(00)00098-9)
- Singer, J. D. (1998). Using SAS PROC MIXED to fit multilevel models, hierarchical models, and individual growth models. *Journal of Educational and Behavioral Statistics*, 23(4), 323–355. <https://doi.org/10.2307/1165280>
- Stockdale, P. H. G. (1970). The development, route of migration, and pathogenesis of *Perostrongylus pridhami* in mink. *Journal of Parasitology*, 56, 559–566. <https://doi.org/10.2307/3277624>
- Stockdale, P. H. G., & Anderson, R. C. (1970). The development, route of migration, and pathogenesis of *Filaroides martis* in mink. *Journal of Parasitology*, 56, 550–558. <https://doi.org/10.2307/3277623>
- Van Goor, J., Herre, E. A., Gómez, A., & Nason, J. D. (2022). Extraordinarily precise nematode sex ratios: adaptive responses to vanishingly rare mating opportunities. *Proceedings of the Royal Society B: Biological Sciences*, 289, Article 20211572. <https://doi.org/10.1098/rspb.2021.1572>
- Wood, S. N. (2017). *Generalized additive models: An introduction with R* (2nd ed.). Chapman and Hall/CRC Press. <https://doi.org/10.1201/9781315370279>

How to cite this article: Pool, R. V., Pons-García, N., Consoli, F., Rivero, M., Bombardi, C., Raga, J. A., & Aznar, F. J. (2024). Fine-scale distribution of the lungworm *Halocercus delphini* in the lungs of the striped dolphin, *Stenella coeruleoalba*: implications about migration pathways and functional significance. *Marine Mammal Science*, e13111. <https://doi.org/10.1111/mms.13111>